

**ANATOMY OF THE VERY TINY:
FIRST DESCRIPTION OF THE HEAD SKELETON OF THE RARE SOUTH
AMERICAN CATFISH *SARCOGLANIS SIMPLEX*
(SILURIFORMES: TRICHOMYCTERIDAE)**

Kerin M. Claeson, James W. Hagadorn, Kyle Luckenbill,
and John G. Lundberg

ABSTRACT

The osteology of *Sarcoglanis simplex*, a rare, miniature South American catfish, is described for the first time based on a single, 17 mm adult specimen that was both cleared and Alizarin-stained, and visualized with microfocus computed tomography (MicroCT). Previously, the internal skeletal features of this species could be predicted based only on conditions observed in its closest relatives within the subfamily Sarcoglanidinae of the Trichomycteridae. The relatively new MicroCT technique successfully revealed fine details of the skeletal morphology of this tiny fish. As predicted, *Sarcoglanis* shares with *Stauroglanis*, *Stenolicmus*, *Malacoglanis*, *Microcambeva*, and *Ammoglanis* an anterior ossification of the palatine and a large posteriorly directed dorsal process on the quadrate. Contrary to predictions, however, the mesethmoid of *Sarcoglanis* does not have the distal ends of the cornua distinctly wider than at their bases, and the anterior margin of the mesethmoid is not convex.

Kerin M. Claeson. The Department of Geological Sciences, The Jackson School of Geosciences, The University of Texas at Austin, Austin, TX, kclaeson@mail.utexas.edu

James W. Hagadorn. Department of Geology, Amherst College, Amherst, MA, jwhagadorn@amherst.edu

Kyle Luckenbill. Department of Ichthyology, Academy of Natural Sciences, Philadelphia, PA, luckenbill@acnatsci.org

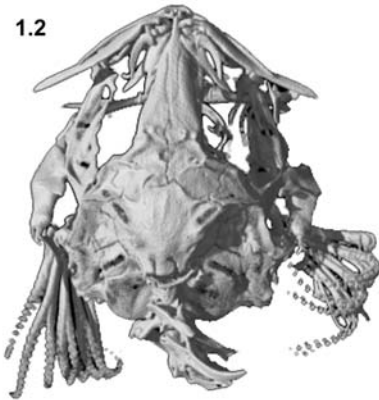
John G. Lundberg. Department of Ichthyology, Academy of Natural Sciences, Philadelphia, PA, lundberg@acnatsci.org

KEYWORDS: miniature, osteology, Sarcoglanidinae, *Microcambeva*, *Stauroglanis*

1.1



1.2



1.3

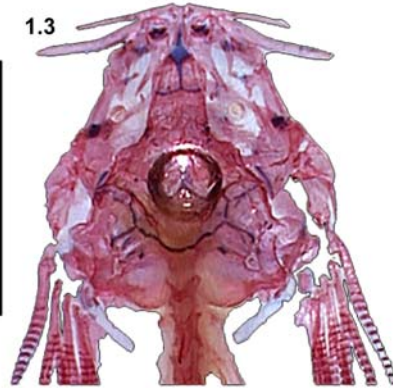


Figure 1. *Sarcoglanis simplex*, ANSP 179212. 1.1 Live *Sarcoglanis* in right lateral view; 1.2 3D model of skull in dorsal view; 1.3 Cleared and stained skull in dorsal view. Air bubble is within neurocranium. Scale bars = 5mm.

INTRODUCTION

Small size and sparse number of specimens raise difficulties for detailed examination of the skeletal anatomy of several groups of fossil and extant fishes. Traditional methods such as maceration or skeletal mounting are not ideal because both increase the risk of losing skeletal elements, and positional relationships are lost or compromised. Comparative morphologic and phylogenetic research on these groups is thus hindered. To address these problems, we used microfocus X-ray computed tomography (MicroCT) to resolve the osteological details needed to conduct comparative anatomical and systematic studies of very small fishes.

Here we report the results of our first case study, an analysis of the rare and diminutive trichomycterid catfish *Sarcoglanis simplex* (Figure 1). *Sarcoglanis simplex* belongs to the trichomycterid subfamily Sarcoglanidinae. This is a small clade of six genera and eight species, all of which are miniature, sand-dwelling catfishes found in rapidly flowing upland streams and rivers. All species of sarcoglanidines have been discovered during the

last 40 years (Myers and Weitzman 1966; de Pinna 1989; de Pinna and Starnes 1990; Costa and Bockmann 1994; de Pinna and Winemiller 2000; Schaefer 2003; Costa et al. 2004). The distinctive characteristics marking this clade and its relationships among trichomycterids were treated by de Pinna (1989), de Pinna and Starnes (1990), Costa (1994), and Costa and Bockmann (1994). The osteology of the nominal genus *Sarcoglanis*, however, was not previously described. The detailed anatomical data presented here are thus critical to testing the phylogeny of the Sarcoglanidinae.

Until recently, *Sarcoglanis* was known only from the holotype specimen collected in the San Gabriel Rapids of the Rio Negro, Brazil (Myers and Weitzman 1966). Expeditions led by researchers at the Academy of Natural Sciences in Philadelphia (ANSP) to the

Essequibo River, Guyana in 2002-2003 and Rio Ventuari, Venezuela in 2004, yielded several additional specimens of *Sarcoglanis*. Representatives of these were made available by M. Sabaj and were identified as *S. simplex* by J. N. Baskin (personal commun., 2004). These newly collected specimens offer us, for the first time, the opportunity to describe the bony skeleton of *Sarcoglanis* and to identify diagnostic characters useful for resolving its phylogenetic affinity.

MATERIALS AND METHODS

One specimen of *Sarcoglanis simplex* (ANSP 179212) was cleared and double-stained with Alizarin Red S and Alcian Blue (Figure 1.3) prior to MicroCT-scanning. This specimen was then wedged in 2% agarose gel and scanned at low voltage (40kV) and high amperage (250A). The agarose gel prevented dehydration, movement, and shrinkage of the specimen during scanning.

An agar wedge was created to stabilize a specimen using the following protocol: A stock solution of 2% agarose gel was heated in the microwave until it was a clear homogeneous liquid.

Agar was then cooled until it was slightly viscous but still clear. Placing the agar into a freezer accelerated cooling. If the agar solution became cloudy, it could not be poured because it tended to clump together. Once slightly viscous, agar was built up around the walls of a small plastic tube in one of two ways, 1) a small amount of liquid agar was poured in a plastic tube that was propped on one side and cooled completely. This step was repeated one or more times creating small shelves against which a specimen could be rested, not allowing it to touch the walls of the tube, or 2) a tube was filled with agar and allowed to cool completely, then a smaller chamber was cut out with a straw. Once an agar chamber was prepared, the specimen was placed into it and slowly covered by warm agar and cooled completely before scanning.

Special care must be taken when scanning 'wet' specimens. It is critical to remove specimens from agar and place them into 70% EtOH (or other curatorial storage medium) within a few days of scanning. The agar remains slippery and relatively brittle when sealed in most mounting tubes for 3-4 days. The agar can be split apart easily allowing the specimen to slide out. If multiple scans are conducted on a single mount, the ends of the tube housing the specimen need to be capped. Capping is typically not enough to prevent dehydration if several days pass between each scan. Agar dehydration can cause a specimen to shift and eventually will make it difficult to remove. In the event that a specimen remains wedged too long, ethanol helps to dissolve the agar. Soaking time in ethanol will vary, but a minimum of one week is suggested. Water and glycerin will not break down the agar.

All scans were conducted on the Skyscan 1172 Microfocus X-radiographic Scanner at Amherst College. Details of scanning parameters are provided in Table 1. MicroCT creates a series of individual X-ray projection images that together form a 360° profile through a specimen. Greyscale values in these images correspond to X-ray attenuation, which varies as a function of variations in density and average atomic number. Greyscale values were determined on a per-specimen basis. Projection images were converted using filtered back-projection into a volume consisting of a stack of X-ray attenuation cross sections, or slices, using the reconstruction software, Cone-Beam Reconstruction v. 2.23 (SKYSCAN, Kontich, Belgium). Dark regions visible in each cross section represented areas of a specimen (i.e., skeletal elements) that are more ossified, and lighter regions

Table 1. Scanning parameters for *Sarcoglanis simplex* scan.

Parameter	Value
Camera Pixel Size	11.70 μ m
CameraXYRatio	0.9800
Incl.in lifting	1.0620 (m/mm)
Source Voltage	40 kV
Source Current	250 A
Number of Rows	2096
Number of Columns	4000
Number of connected scans	3
Number of lines to be reconstructed	1579
Image Pixel Size	2.48 μ m
Object to Source	45.710 mm
Camera to Source	215.722 mm
Optical Axis	1246 line
Filter	No filter
Depth	16 bits
Screen LUT	0
Exposure	1767 ms
Rotation Step	0.300 degrees
Frame Averaging	On = 3
Random Movement	On = 20
Use 360 Rotation	Yes
Geometrical Correction	On
Median Filtering	On
Flat Field Correction	On
Rotation Direction	CC
Scanning Trajectory	Round
Type Of Motion	Step and shoot

typically correspond to soft tissues such as muscle, ligament, or organs, or to voids within samples. Each slice was inverted in color for analysis with the 3D imaging software VGStudio MAX v.1.2.1 (Volume Graphics, Heidelberg, Germany) at The University of Texas at Austin and the Academy of Natural Sciences, Philadelphia. Using thresholding, a range of greyscale values observed on individual bones were identified and digitally isolated from cross-sectional slices. Three-dimensional volume models of structures within the slice volume were produced and volume rendered. In regions where bones are poorly ossified or thin, there are gaps in volume renderings. Some anatomical observations noted in the text will, therefore, not match one-to-one with the figures. Descriptions of osteological features are based on the single C&S specimen and scan data of this specimen. The terminology proposed by de Pinna (1989) is followed. Animations of 3D models were produced using VGStudio MAX and Quicktime Pro.

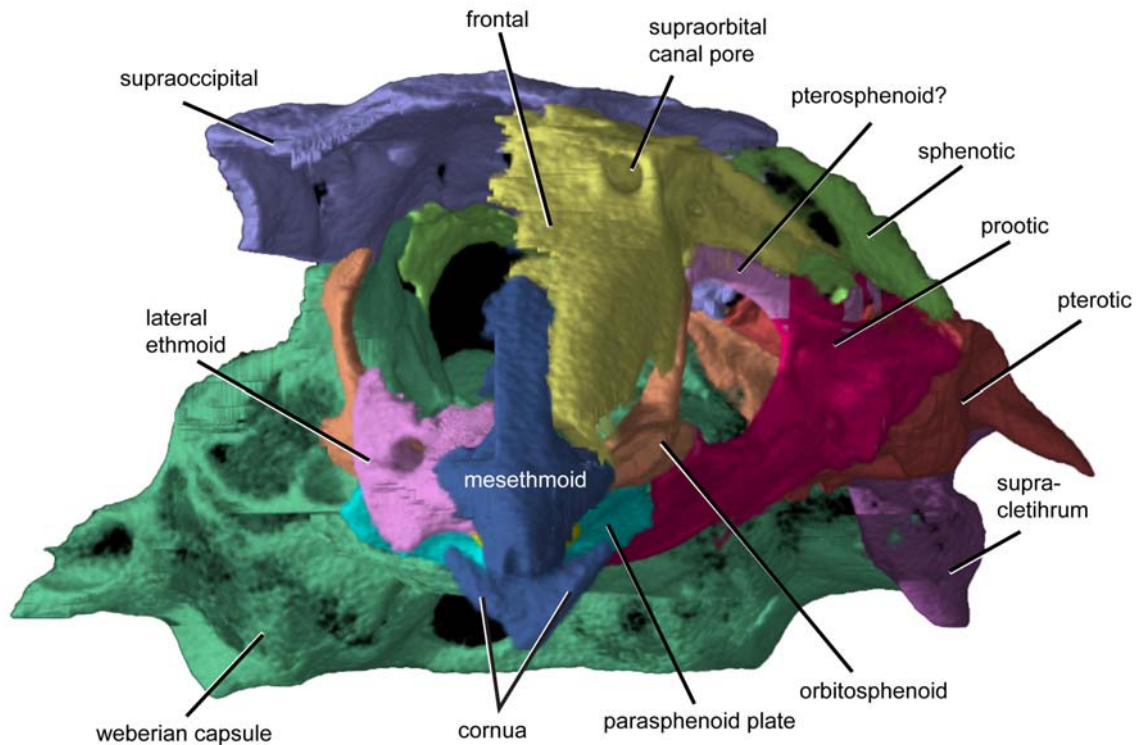


Figure 2. Anterior view of 3B model of *Sarcoglanis simplex* neurocranium, ANSP 179212. The right side of model was segmented away for this figure. Left lateral ethmoid was segmented away to show orbitosphenoid. See Figure 9 for cutaway in this plane. Scale bar = 1mm.

RESULTS

The specimen of *Sarcoglanis simplex* analyzed for this pilot study was only 17 mm standard length. The head skeleton is 5.5 mm long and 5 mm wide across the widest part of the skull (from left to right opercle) giving the head skeleton an almost spherical overall shape. The delicate jaw, suspensory, branchial, and pectoral girdle elements are moveably (kinetically) articulated to a pear-shaped neurocranium (Figure 2).

Neurocranium. The mesethmoid is a long bone located along the midline of the snout (Figures 2-6). It is slender anteriorly, and its posterior third widens at its joint with the lateral ethmoids. The cornua of the mesethmoid are curved anteroposteriorly creating a v-shaped notch on the midline (Figure 2). Lateral ethmoids are situated postero-laterally ventrally to the mesethmoid, ventral to the frontal-mesethmoid joint and anterior to the orbitosphenoid (Figure 2). The lateral ethmoids are laterally expanded and cuplike. Lateral ethmoids are opened dorsally but covered by the anterior process of the frontal. The lateral ethmoids are much wider than the frontal process of the mesethmoid (Figures 3 and 4). Posterior to the lateral ethmoids

is the orbitosphenoid that contributes to the floor and anterior sidewalls of the neurocranium. The floor of the orbitosphenoid is relatively thin (Figures 3 and 4). There is a sharp notch posteriorly on the orbitosphenoid where the parasphenoid plate attaches. The neck of the parasphenoid extends anteroventrally to the orbitosphenoid and contacts the posteriormost portion of the lateral ethmoids and median vomer (Figure 4). Along the parasphenoid neck, is a well-developed longitudinal crest that starts on the parasphenoid plate and terminates behind the vomer. The head of the kite-shaped vomer is ventral to the ethmoid cartilage and a deep trench in the mesethmoid. The vomer in *Sarcoglanis* is long but relatively narrower than the vomer in *Stauroglanis* (de Pinna 1989: figure 5).

Paired frontals are located anterodorsally (Figures 2 and 3; Figure 7). A wide supraorbital canal is present along the margin of posteriormost third of each frontal, and a canal pore is present at the anterior extremity of the supraorbital canal on the frontal. The supraorbital laterosensory canal continues along the margin of the sphenotic (Figure 3; Figure 8). The left and right supraorbital canals meet medially as in *Microcambeva ribeirae*

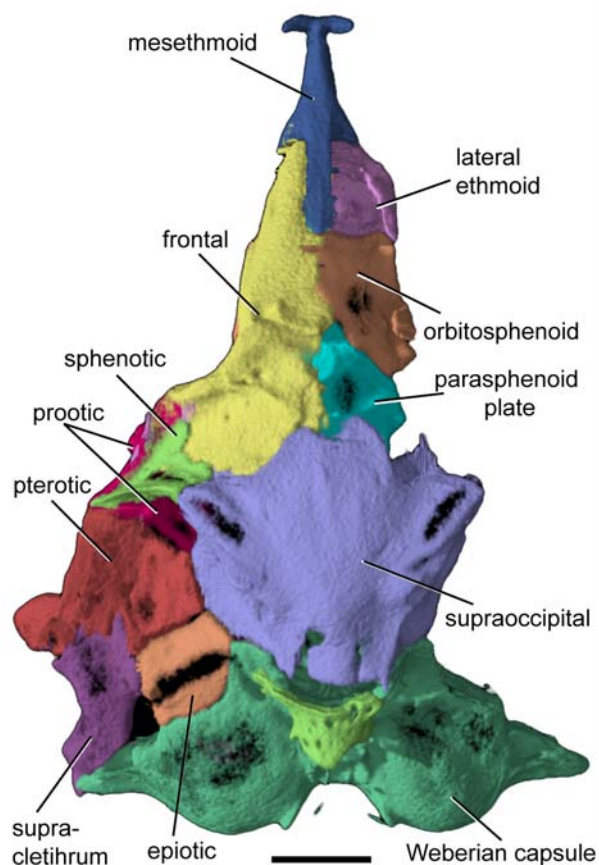


Figure 3. Dorsal view of 3D model of *Sarcoglanis simplex* neurocranium, ANSP 179212. The right side of model and left lateral ethmoid were segmented away for this figure. See Figure 7 for 360 degree rotation. Scale bar = 1mm.

(Costa et al. 2004, figure 3). The anterior mesethmoid process of the frontal is narrow and extends approximately half the length of the mesethmoid. The posteriormost third of the frontals widens abruptly behind the orbit and suture to one another. There is no anterior cranial fontanelle between the frontals, though a remnant fontanelle may be present in the form of a small circle between the frontal suture (Figure 1.2). The posterior margin of the frontals contacts the anterior margin of the supraoccipital that also lacks a midline fontanelle. Posterolaterally, the frontal contacts the sphenotic part of the compound sphenotic-prootic bone.

The supraoccipital is broad across its joint with the frontals and the sphenotics (Figures 2 and 3). A short shelf lies ventral to the posterior end of the frontal. Two anterolaterally diverging crests on the supraoccipital are continuous with the coronal crest of the sphenotic. Absent from the neurocranium of *S. simplex* are any anterolateral openings

(de Pinna 1989). Areas of weak ossification, however, are present above the supraoccipital crests (Figure 3). Ventrally, there are elongate, slit-like gaps formed by the supraclathrum and Weberian complex (Figure 4).

The supraorbital canal continues from the frontal through the sphenotic part of the sphenotic + prootic complex and connects to the postotic canal in the pterotic (Figure 9). De Pinna (1989) recognized three bones in this complex: the sphenotic, prootic, and pterosphenoid. The postotic canal continues through to the supraclathrum. The sphenotic bone is small dorsally. Ventrolaterally, the sphenotic contacts the prootic. The prootic extends ventrally contacting the entire dorsolateral margin of the parasphenoid plate and the anterior-most margin of the basioccipital-Weberian complex (Figures 4 and 5). The prootic is weakly ossified ventrally. Posterior to the prootic + sphenotic complex is the pterotic, which contributes to the lateral walls of the neurocranium. The pterotic contacts the sphenotic anterodorsally, the prootic anteriorly, the supraoccipital dorsally, the epiotic posterodorsally, and the supraclathrum posteriorly. Anterior to the supraclathrum is a short, thick process that extends anterodorsally off the lateral wall of the pterotic. We were unable to differentiate a separate pterosphenoid. There is, however, a small bridge of bone extending anterodorsally from the prootic to the orbitosphenoid contributing to a foramen for the passage of the optic, trigeminal, and facial nerves (Figures 5.1 and 5.2: rendered light pink). This bridge of bone may be the remnant of the pterosphenoid. Posterior to the pterotic compound is the supraclathrum. The supraclathrum is long and poorly ossified laterally. There is a small canal pore at the posterior limit of the supraclathrum adjacent to the lateral projection off the Weberian capsule (Figure 5).

Jaws. The premaxilla is located lateral to the mesethmoid cornua. It is an exceptionally long, slender, and toothless bone approximately three-quarters the length of the maxilla. The mesethmoid process of each premaxilla is short and hooked around its cornua, articulating both in front of and behind the cornua (Figure 6). Anteroventral to the mesethmoid process of the premaxilla is a small shelf that projects out under the cornua of the mesethmoid. There are two small projections of equal size on the proximal half of the premaxilla that are separated by a c-shaped gap (Not shown in Figure 6, see Figure 9). This gap articulates with the premaxillary process of the maxilla. Distal to the maxillary articulation, the premaxilla tapers to a

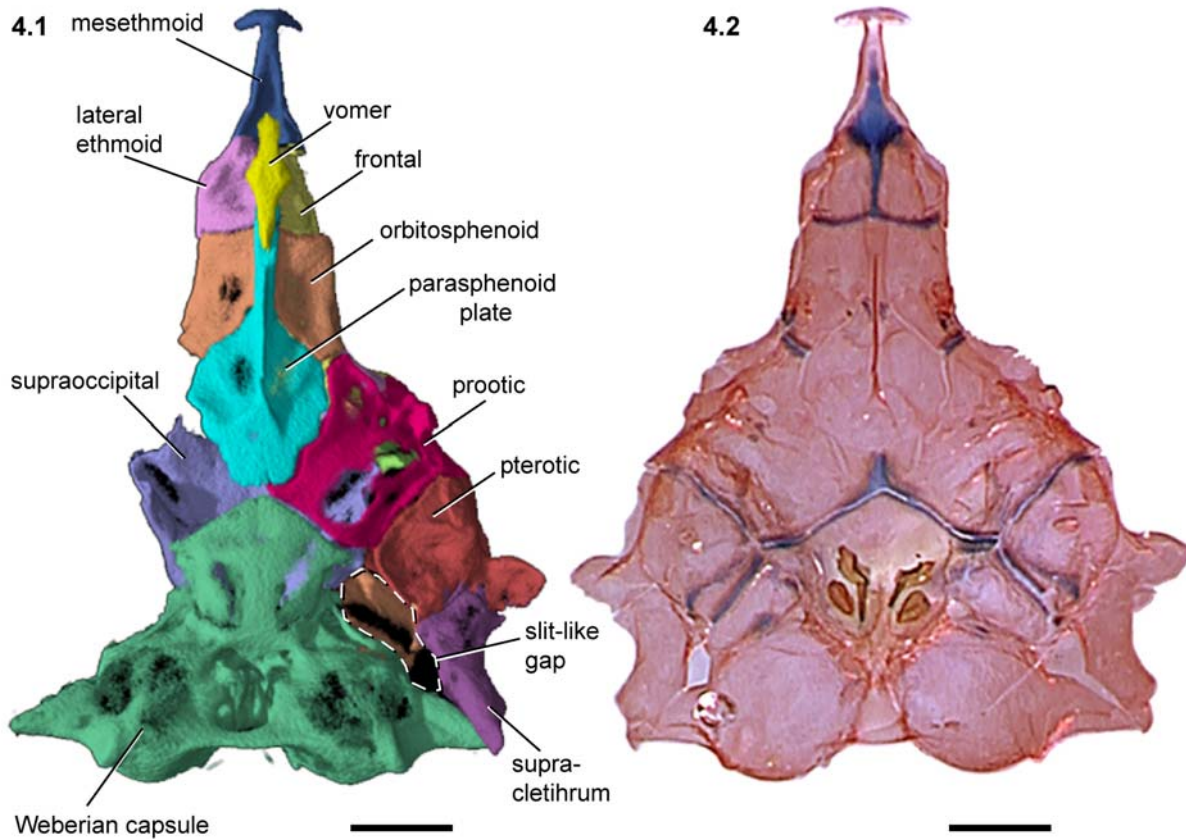


Figure 4. Ventral view of *Sarcoglanis simplex* neurocranium, ANSP 179212. 4.1 3D model. The right side of the model has been segmented away. The left lateral ethmoid has been segmented away to show the frontal; 4.2 Complete ventral view of C&S specimen. See Figure 7 for 360 degree rotation. Scale bars = 1mm.

point. The distalmost end of the premaxilla is pointed and flattened anteroposteriorly.

The maxilla is greatly enlarged. Proximally, the maxilla is laterally compressed. A short square process articulates with the mesethmoid posterior to the mesethmoid process of the premaxilla. The main articulation of the maxilla is with the large anterior palatine cartilage that fills the space between most the space between these bones (not shown). The premaxillary process of the maxilla is triangular and contributes to the deepest portion of the maxilla. Distal to this process the maxilla tapers gradually and twists slightly.

The palatine is located posterior to the maxilla and lateral to the mesethmoid (Figure 6). The palatine articulates with a slight anterolateral concavity of the lateral ethmoid (Figures 5.1 and 6). The body of the palatine is rectangular with a long process projecting from the dorsolateral corner. There is a small anterior ossification of the palatine present. The lateral margin of the palatine is concave and continues from the short maxillary process of

the palatine to the long, pointed posterior process. The maxillary process articulates in a facet on the internal side of the maxilla. The posterior process is shorter than that in *Microcambeva* and thinner than that in *Stauroglanis*.

Suspensorium and operculars. There is a minute cylindrical metapterygoid located anterodorsal to the quadrate (Figure 10). The quadrate is relatively stout and is approximately the same length as the preopercles. There is a robust, round process that projects anteroventrally and articulates with the lower jaw, not treated in this analysis. Dorsal to this articular process is the hyomandibular process. The hyomandibular process is posteriorly recurved. It has two smaller processes that project from it. The anterior one articulates with the metapterygoid cartilage, and the posterior one comes close to but does not articulate with the hyomandibula. The hyomandibula is the largest bone in the suspensorium. It is roughly rectangular and flat. There is a short, wide process associated with the

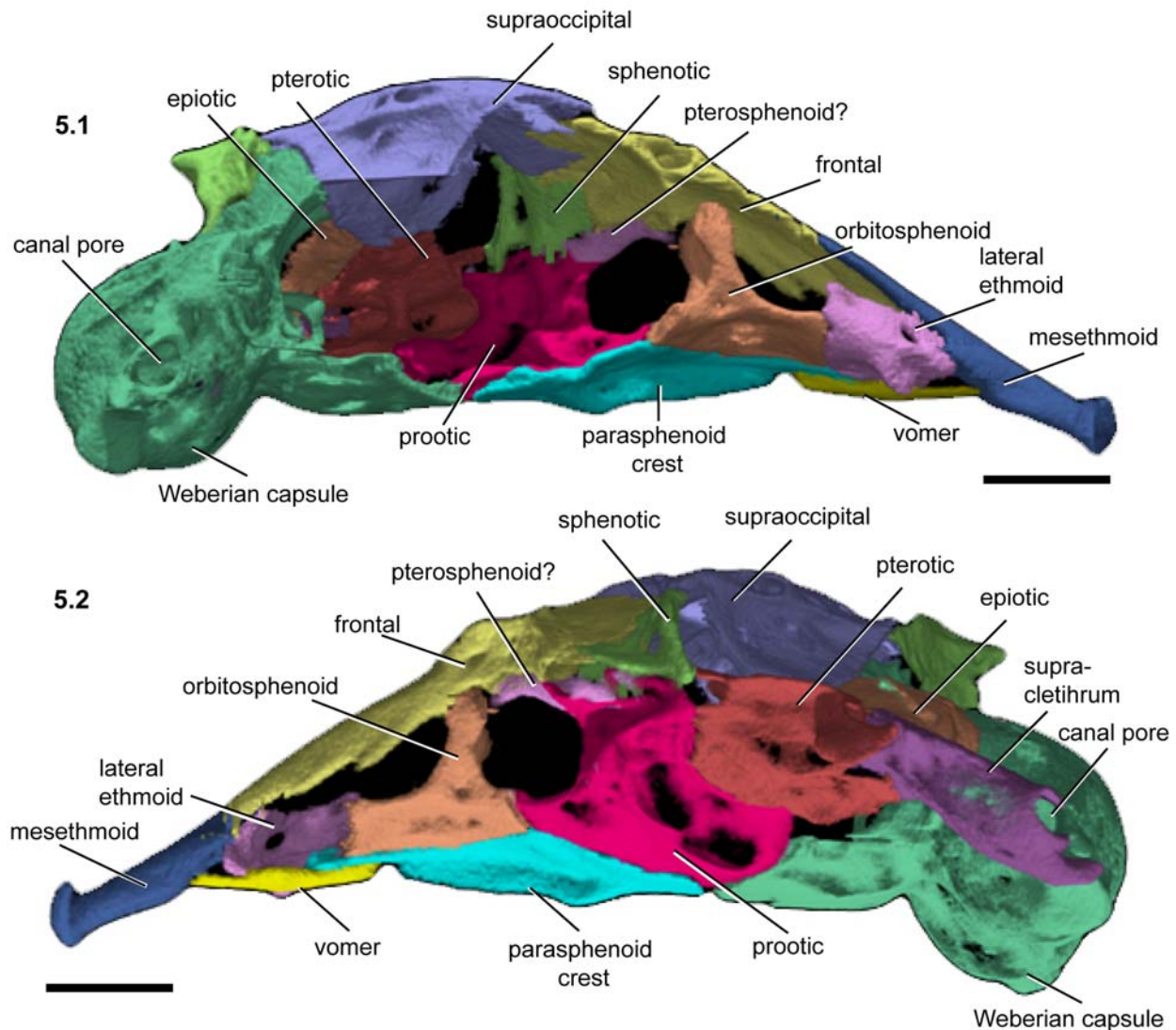


Figure 5. Three dimensional model of *Sarcoglanis simplex* neurocranium, ANSP 179212. 5.1 Right medial view. The right side of model and left lateral ethmoid have been segmented away; 5.2 Left lateral view. See Figure 7 for 360 rotation. Scale bars = 1mm.

hyomandibular process of the quadrate. Across the body of the hyomandibula is a well-defined ridge (Figure 10.1-2). This ridge lacks a strong pointed process like that in *Stauroglanis* (de Pinna 1989).

The preopercle is a long, boomerang-shaped bone. It partially overlies the synchondral articulation between the quadrate and the hyomandibula in lateral view (Figure 10.1-2). The preopercle is strongly associated with these bones. Ventrally, it contacts the interopercle. The main body of the interopercle is square, but a posteriorly directed process is present on the posteroventral corner. There are no odontodes present on the interopercle. The opercle is approximately the same length as the hyomandibula. Posteriorly, there is a long

process with a robust distal end from which three opercular odontodes project. Anteriorly, there is a pointed process that associates with a notch in the interopercle. A third, flat, well-developed process is present midway along the opercle that is aligned with the hyomandibular ridge and is likely the attachment site of the dilatator operculi muscles that in these trichomycterids is involved in elevating the patch of odontodes (Figure 10.1). This process is not present in *Microcambeva* and *Stauroglanis*; however, both these fishes have a shorter process that is continuous with the hyomandibular edge of the opercle (de Pinna 1989; Costa et al. 2004).

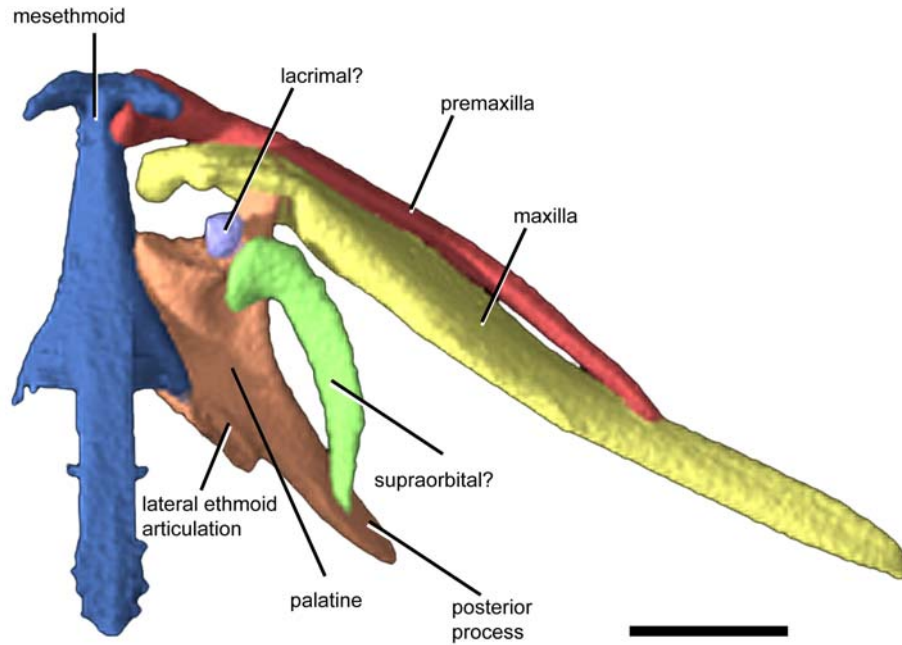


Figure 6. Dorsal view of 3D model of the right side of the snout region in *Sarcoglanis simplex*, ANSP 179212.

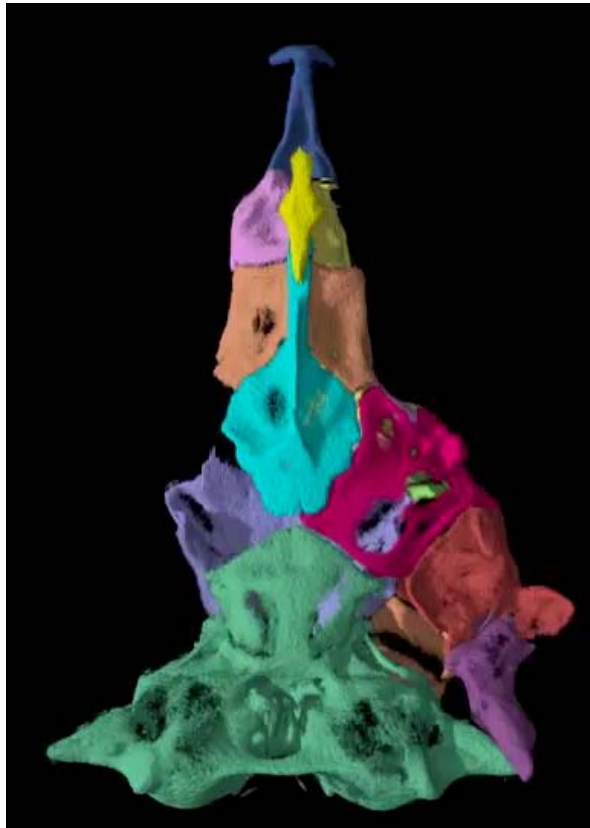


Figure 7. 360 degree rotation of segmented 3D model of *Sarcoglanis simplex* neurocranium, ANSP 179212. The right side of model and left lateral ethmoid have been segmented away. Anterior is up.

DISCUSSION

Hypothesized sarcoglanidine relationships were proposed by de Pinna (1989, figure 18, p. 26), de Pinna and Starnes (1990) and Costa and Bockmann (1994, figure 7, p. 727), but the most recent and extensive phylogeny is that of Costa (1994, figure 7, p. 213). Sarcoglanidinae and Glanapteryginae are hypothesized to be sister taxa because they share a posteriorly directed dorsal process on the quadrate, a large anteriorly directed dorsal process on the hyomandibula, a reduced vomer, and are all miniature (de Pinna 1989; Costa and Bockmann 1994). *Sarcoglanis* shares with other members of the Sarcoglanidinae and Glanapteryginae these four synapomorphies.

The Sarcoglanidinae are separated from the Glanapteryginae by three apomorphies (Costa and Bockmann 1994). Our analysis of *Sarcoglanis* indicates that this taxon shares with the other members of Sarcoglanidinae a pointed slender lateral process of the premaxilla, an enlarged maxilla, and rounded ventral expansion on the premaxilla. *Sarcoglanis* is thought to be the sister taxon to *Malacoglanis* (Sarcoglanidinae) based on seven synapomorphies (Costa 1994). Our integrated CT- and C&S-based analysis supports this phylogenetic relationship, confirming the osteological characters proposed by Costa (1994) including the presence of elongate pectoral fins and a lack of premaxillary teeth.

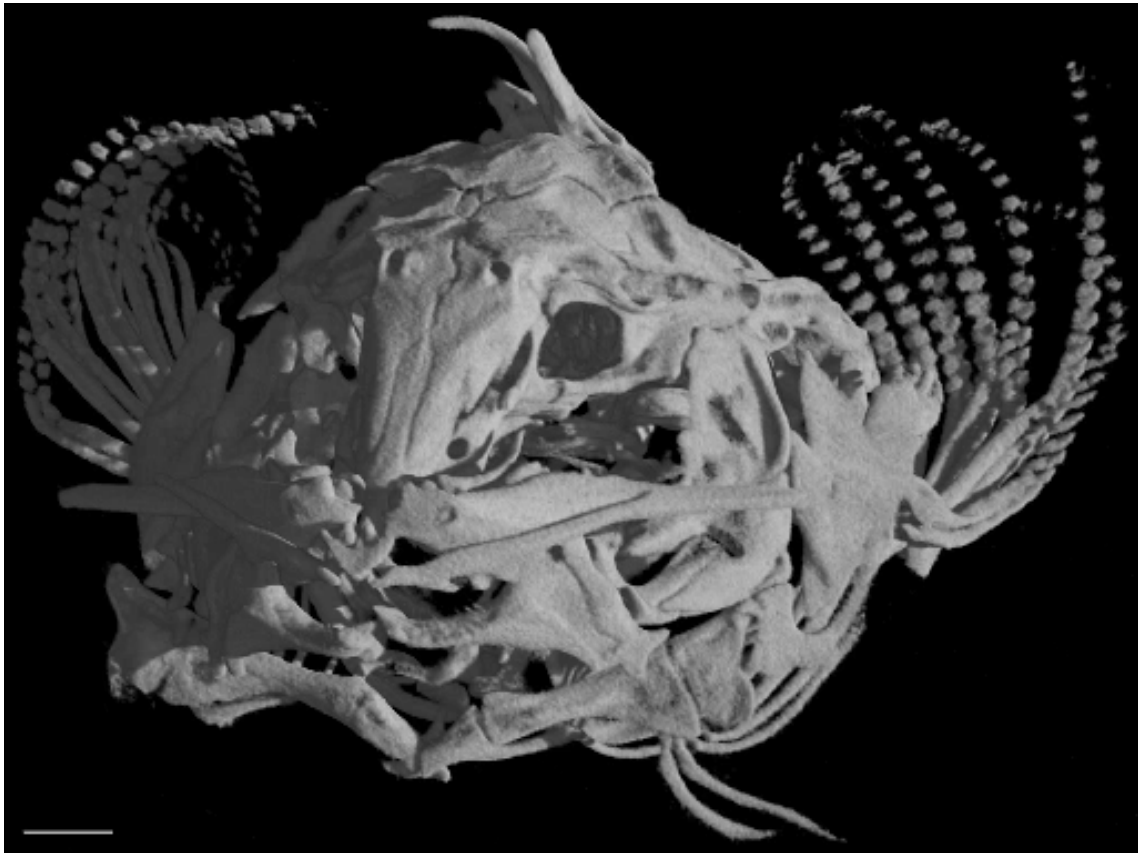


Figure 8. Anterior view cutaway of unsegmented 3D model of of *Sarcoglanis simplex* neurocranium, ANSP 179212.

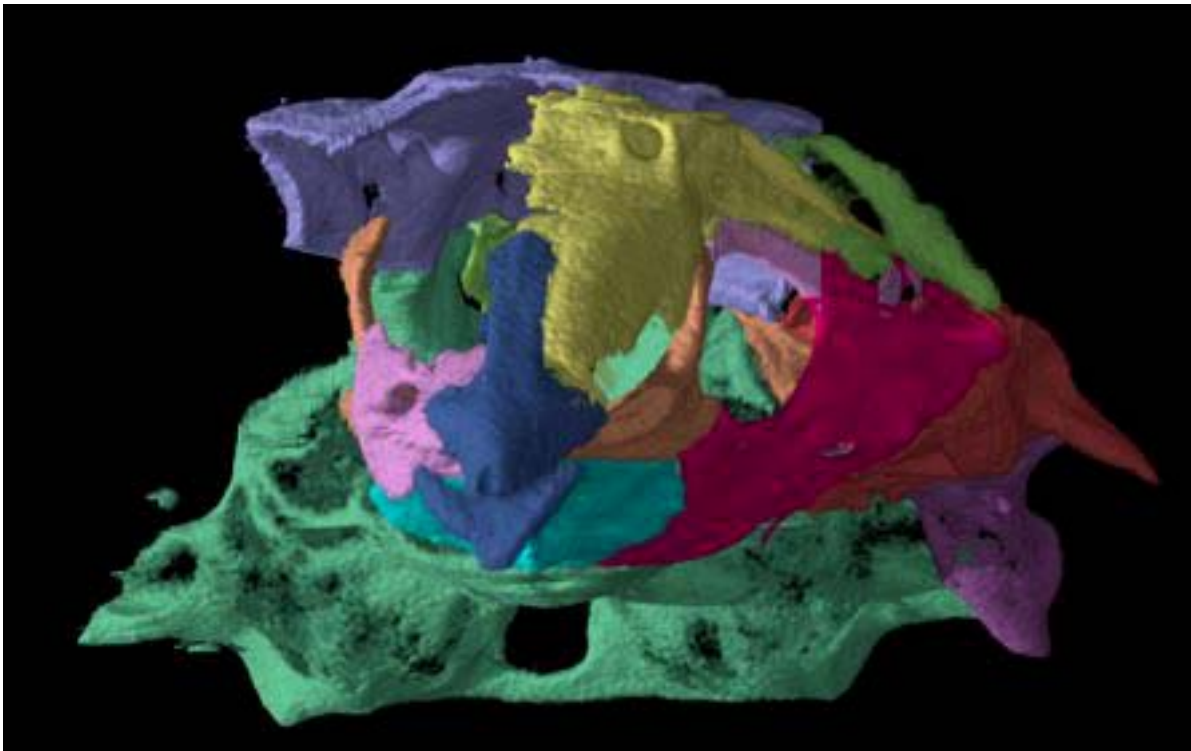


Figure 9. Anterior view cutaway of segmented 3D model of of *Sarcoglanis simplex* neurocranium, ANSP 179212. The right side of model and left lateral ethmoid have been segmented away.

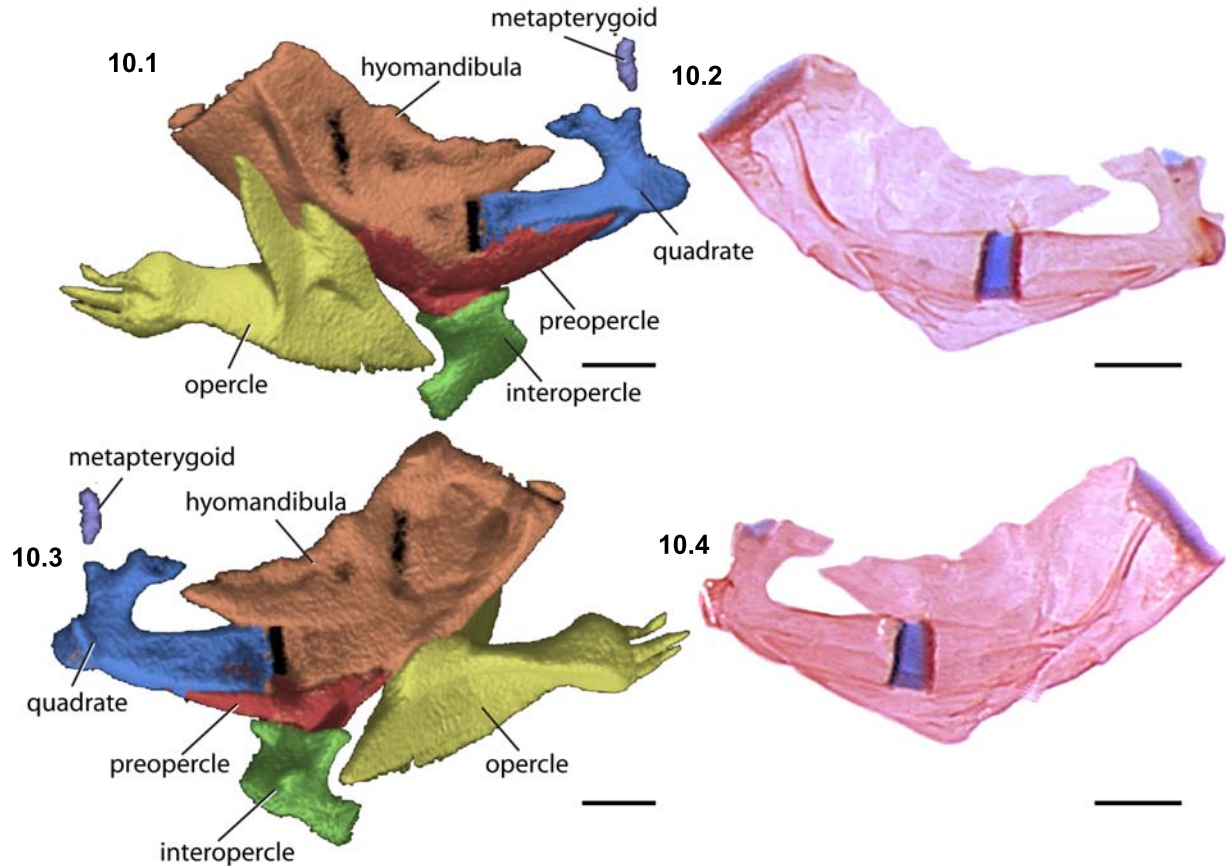


Figure 10. Suspensorium of *Sarcoglanis simplex*, ANSP 179212. 10.1 3D model in right lateral view; 10.2 C&S image in right lateral view; 10.3 3D model in right medial view; 10.4 C&S image in right medial view. Scale bar = 1mm.

CONCLUSIONS

Sarcoglanis is an odd, but remarkable, derived sarcoglanidine catfish that requires further investigation before we can understand its suite of unusual characters. Using MicroCT and new mounting techniques described herein, we can now begin to more rigorously characterize the skeletal anatomy of extremely small and rare vertebrates, including wet museum specimens. For diverse groups like catfish, a new opportunity arises to begin to efficiently assess their ontogenetic, ecological, and evolutionary history.

ACKNOWLEDGEMENTS

We thank the coordinators of the Digital Symposium at the 66th Annual Society of Vertebrate Paleontology Meetings for allowing us to present preliminary results from this study. We also thank C.J. Bell for his comments on the manuscript. D. Kelly and M. Manning constructed post scan data sets. Funding was provided by NSF EAR 0236775,

NSF DEB 0315963, SICB Student Support, and the All Catfish Species Inventory.

REFERENCES

- Costa, W.J.E.M. 1994. A new genus and species of Sarcoglanidinae (Siluriformes: Trichomycteridae) from the Araguaia basin, central Brazil, with notes on subfamilial phylogeny. *Ichthyological Exploration of Freshwaters*, 5:207-216.
- Costa, W.J.E.M., and Bockmann, F.A. 1994. A new genus and species of Sarcoglanidinae (Siluriformes: Trichomycteridae) from southeastern Brazil, with a re-examination of subfamilial phylogeny. *Journal of Natural History*, 28:715-730.
- Costa, W.J.E.M., Lima, S.M.Q., and Bizerril, C.R.S.F. 2004. *Microcambeva ribeirae* sp. n. (Teleostei Siluriformes: Trichomycteridae): a new sarcoglanidine catfish from the Rio Ribeira do Iguape basin, southeastern Brazil. *Zootaxa*, 563:1-10.
- de Pinna, M.C.C. 1989. A new sarcoglanidine catfish, phylogeny of its subfamily, and an appraisal of the phyletic status of the Trichomycterinae (Teleostei, Trichomycteridae). *American Museum Novitates*, 2950:1-39.

- de Pinna, M.C.C.. and Starnes, W.C. 1990. A new genus and species of Sarcoglanidinae from the Río Mamoré, Amazon Basin, with comments on subfamilial phylogeny (Teleostei, Trichomycteridae). *Journal of Zoology (London)*, 222:75-88.
- de Pinna, M.C.C., and Winemiller, K.O. 2000. A new species of *Ammoglanis* (Siluriformes: Trichomycteridae) from Venezuela. *Ichthyological Exploration of Freshwaters*, 11:255-264.
- Myers, G.S., and Weitzman, S.H. 1966. Two remarkable new trichomycterid catfishes from the Amazon Basin in Brazil and Colombia. *Journal of Zoology (London)*, 149:277-287.
- Schaefer, S.A. 2003. Relationships of *Lithogenes villosus* Eigenmann, 1909 (Siluriformes: Loricariidae): Evidence from high-resolution computed microtomography. *American Museum Novitates*, 3401:1-55.